Nonlinear Behavior and Design of Mid- to High-Rise Diagrid Structures in Seismic Regions

ESMAEEL ASADI and HOJJAT ADELI

ABSTRACT

The aesthetics and structural advantages of the diagrid structural system have made it an attractive choice for many buildings across the world, including several notable high-rise building structures built in recent years. This paper presents an investigation of nonlinear behavior and design of mid- to high-rise steel diagrid structures. Weight, story drift, fundamental period, lateral stiffness, and sequence of plastic hinge formation in steel diagrids are studied and compared with corresponding moment-resisting frames and concentrically braced frames. To improve the nonlinear behavior and increase the collapse load capacity of diagrid structures in high seismic regions, practical design guidelines are proposed by using virtual work/energy diagrams and by performing nonlinear static analysis. So far, the diagrid system has been used mostly in the design of tall buildings in the range of 20 to 100 stories. A conclusion of this research is that the diagrid system can also be an efficient and economical structural system for mid-rise buildings in the 8- to 15-story range.

Keywords: diagrid, mid-rise, high-rise, steel, seismic.

INTRODUCTION

In recent years, there have been a number of attempts to augment the three main and commonly used structural systems for resisting the horizontal loads due to wind and earthquake loading—moment-resisting frames, braced frames, and shear walls—with innovative systems. Reviews of innovative high-rise building structures with an eye on sustainability are presented by Wang and Adeli (2014) and Rafiei and Adeli (2016). Among them is the diagrid system known to be a descendant of braced frames. While most engineers attempted to hide braced frames within the interior or façade of buildings, a few made it an integral part of the building facade. An early and notable example is the 100-story John Hancock Building in Chicago built in the late 1960s, where large braced frames were used on the exterior perimeter of the building not only to withstand the lateral loads, but also to improve the building's outer face aesthetic (Moon et al., 2007).

The word *diagrid* is a combination of *diagonal* and *grid* used for the first time by pioneering Russian architect Vladimir Shukhov for the world's first hyperboloid structure built in 1896 (Boake, 2014). The first application of diagrid in buildings appears to be the IBM building (now called the United Steelworkers Building) in Pittsburgh built in 1965 (Moon et al., 2007). Early researchers were concerned mostly with the analysis of diagonal grids in general, not specifically for tall buildings. For example, Subaramanian and Subaramanian (1970) presented partial difference equations for the slope-deflection method to find in-plane deflection of a simple uniform rectangular diagrid. Grigorian and Kashani (1976) proposed formulas to find the collapse load of rectangular diagonal grids and suggested methods for their analysis and design.

The aesthetics and structural advantages of diagrid have made it an attractive choice for many buildings across the world, such as the 42-story Hearst Building in New York, the 41-story Swiss Re Building in London (Ali and Moon, 2007), and the 54-story CCTV headquarters in Beijing. The major difference between diagrids and braced frames is the omission of vertical members, or columns, from the exterior structure. In diagrids, lateral forces due to wind or earthquake are transferred primarily via axial forces in diagonal members; bending moment makes a small contribution to the design of the diagonal section.

In the past decade, extensive research has been done on the design and diagonal configurations of diagrids in tall buildings. Moon et al. (2007) and Moon (2008) present a stiffness-based approach for the preliminary design of each diagonal member. They also study the effect of the angle of the diagonals with the horizontal axis on the overall stiffness of the frame. Zhang et al. (2010) propose gradually varying angles for diagrids and report the most efficient varying angle for diagrids in terms of the aspect (height-to-width) ratio. Kim and Lee (2012) study the nonlinear static and time-history dynamic behavior of diagrids and recommend

Esmaeel Asadi, Department of Civil Engineering, Case Western Reserve University, Cleveland, OH. Email: exa187@case.edu

Hojjat Adeli, Department of Civil, Environmental, and Geodetic Engineering, The Ohio State University, Columbus, OH. Email: adeli.1@osu.edu (corresponding)

Paper No. 2017-05R2

a diagonal angle between 60° and 70° as the most advantageous angle for most diagrid structures.

Kim and Lee (2010) report progressive collapse resistance of tubular diagrid high-rise building structures as generally high, while conventional tubular structures show a slightly larger resistance. They highlight the importance of corner diagonals against progressive collapse. A review of diagrid structures as a sustainable and efficient structural system is presented in a recent article by Asadi and Adeli (2017).

The diagonal-angle, the angle of diagrid members with the horizontal line in practice, is determined based on architectural and aesthetic requirements, story heights, span length, and lateral load intensity and distribution. Several parametric studies have been conducted on the optimal diagonal angle, which are discussed in Asadi and Adeli (2017).

This research aims to encourage structural designers and stakeholders to look into an innovative structural system with unique properties for their steel structures. The goal of this research is to assess diagrid characteristics and behavior in mid- to high-rise buildings and explore practical solutions for their design shortcomings. Structural and economic aspects of typical diagrids are compared with moment-resisting frames (MRF) and concentrically braced frames (CBF) using linear analysis to study their story drift and modal response and nonlinear analysis to evaluate their performance and failure mechanism. Design guidelines are presented for the seismic design of steel diagrid structures in high seismic regions, which can be used in future AISC and ASCE seismic provisions for the diagrid system.

EXAMPLE STRUCTURES

Model Specifications

Diagrids provide considerable stiffness against lateral loads due to wind and earthquake loads and are attractive for tall buildings (Ali and Moon, 2007). Providing appropriate lateral stiffness is also important for mid-rise buildings in seismic regions—especially for those with large aspect ratios. Therefore, in this research, inelastic seismic behavior of mid- to high-rise steel diagrid buildings is studied. Three groups of office buildings with similar plans are considered with the number of stories equal to 8, 15 [Figure 1(a)], and 30 [Figure 1(b)]. The first two groups represent mid-rise buildings. The third group has a similar elevation but a different plan shown in Figure 1(b). The elevation and perspective view of the 8-story structure are shown in Figures 2(a) and 2(b), respectively. Each structure of the first and second groups consists of a core with four columns at its corners and two outer spans on either side connecting the diagrids to the core [Figure 1(a)]. The third group has a set of 25 central columns arranged on a larger square plan [Figure 1(b)]. A story height of 11.5 ft (3.5 m) is used for all models similar to previous studies (Zhang et al., 2010; Kim and Lee, 2012). Three diagrid patterns with diagonal angles of approximately 45°, 63° and 72° with the horizontal are studied. The structures are labeled by using the number of stories and their diagonal angle. For instance, structure 15-63 refers to a 15-story diagrid structure with a diagonal angle of 63°, as shown in Figure 2(a).

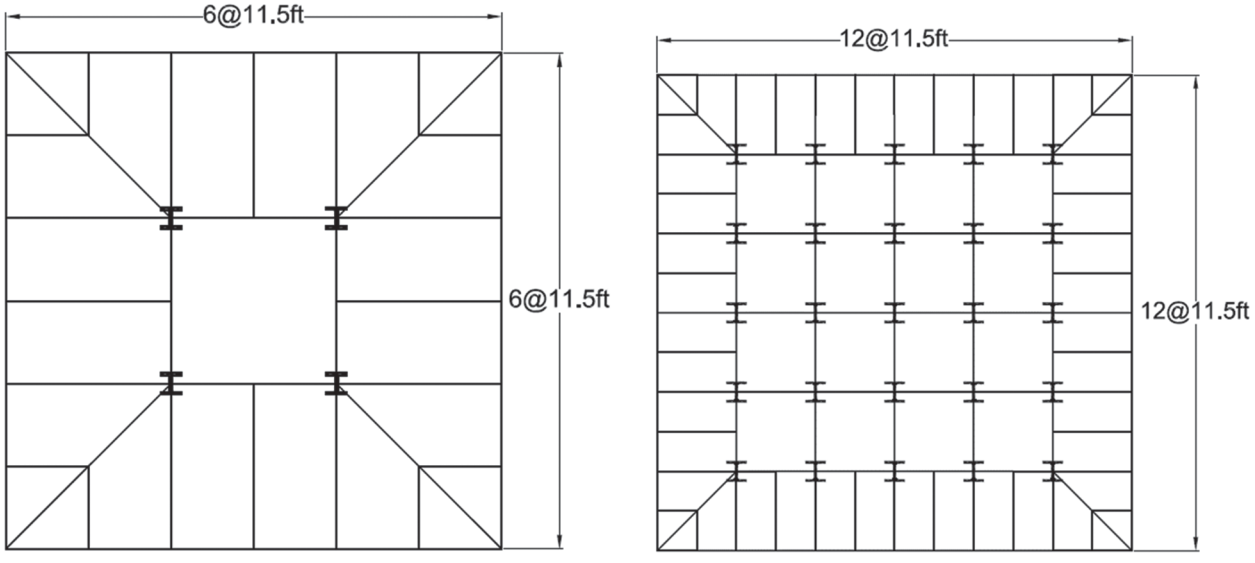

(a) *(b)*

Fig. 1. Typical floor plan for (a) 8- and 15-story buildings and (b) 30-story buildings.

Design of Structures

All models are designed in accordance with the 2016 AISC *Specification* (AISC, 2016b) and the 14th Edition AISC *Steel Construction Manual* (AISC, 2011) utilizing the Load and Resistance Factor Design (LRFD) approach using the software package SAP2000. The response modification, R, factor is assumed to be 3.0, similar to previous studies (Kim and Lee, 2010, 2012; Kim and Kong, 2013). This conservative assumption does not mean that the R factor of steel diagrids is equal to 3.0. Note that ASCE/SEI 7 (2010) does not permit structural systems with $R \leq 3.0$ to be constructed in a site with Seismic Design Category D to F. The AISC *Seismic Provisions* (AISC, 2016a) are not used for the design of diagrid frames because they are not recognized by the current design code, but the amplified seismic load combinations are considered for the internal columns. The following two load combinations with overstrength factors from ASCE/SEI 7, Section 12.4.3.2 are included in design load combinations for the columns:

$$(1.2 + 0.2S_{DS})D + \Omega_o Q_E + L \quad (1)$$

$$(0.9 - 0.2S_{DS})D + \Omega_o Q_E \quad (2)$$

where D, L, Q_E, Ω_o and S_{DS} are the effects of dead and live load and horizontal seismic forces, overstrength factor assumed equal to 3.0, and design spectral response acceleration parameter at short periods, respectively. MRF and CBF models are checked according to AISC *Seismic Provisions* Section E2 (Intermediate Moment Frames) and F2 (Special Concentrically Braced Frames) (AISC, 2016a). SAP2000 has been used by a number of other diagrid system researchers in recent years in a similar fashion (Moon et al., 2007; Kim et al., 2010; Kim and Lee, 2012; Kim and Kong, 2013).

Standard W-sections are used for all diagonals, beams and columns. Following practical considerations, the same diagonals and column sections are used for every three stories across the width. Diagonal connections are moment-resisting connections, and the connections of the columns of MRF and CBF and diagonals of diagrids to the foundation are considered to be fixed except for the central columns, where a hinged condition is chosen so that those columns do not carry any unintended lateral loaded.

Diagonal members are designed to withstand both lateral and gravity loads, while the core columns are designed to carry dead and live loads only. All design loads are calculated per ASCE/SEI 7 for an office building located in southern California, near Los Angeles city, with S_s (spectral response acceleration at 0.2 sec) and S_1 (spectral response acceleration at 1 sec) of 2.461g and 1.127g, respectively. Where permitted by ASCE/SEI 7, the equivalent lateral force (ELF) procedure is used as the method of seismic analysis. In other cases, the modal response spectrum analysis is also carried out to find the critical base shear as required. For wind loads, Exposure Category C and wind speed of 110 mph are used according to the location of the structures. Floors are reinforced concrete slabs with a thickness of 6 in. A total uniform dead load of 85 psf plus a live load of 50 psf are applied on all floors except the roof. For the roof, the dead load is the same but the live load is reduced to 20 psf. The ASCE/SEI 7 requirements for story drift are checked during the design process.

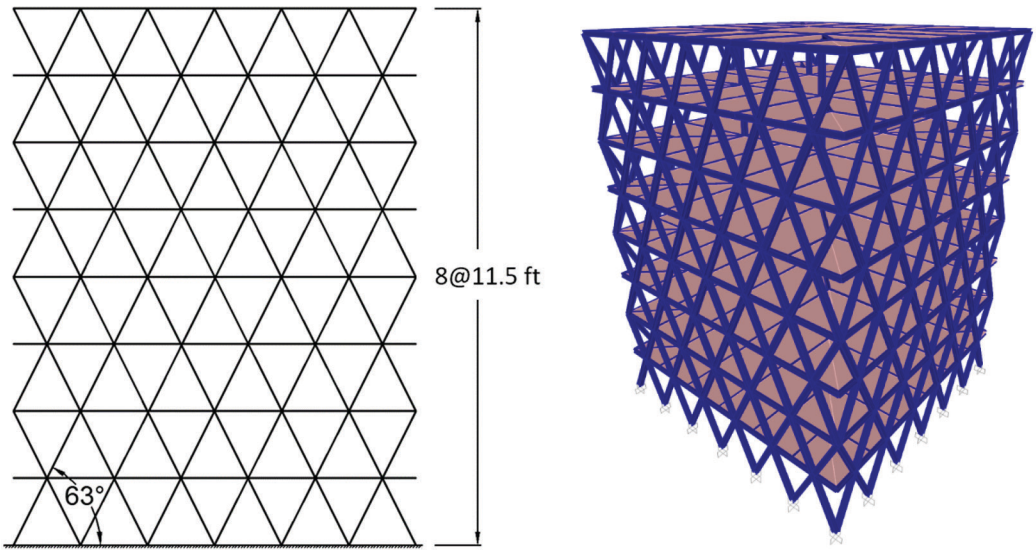

Fig. 2. The 8-63 model (a) elevation and (b) perspective view.

ELASTIC AND INELASTIC BEHAVIOR OF DIAGRIDS

In this section, the elastic internal force distribution and nonlinear behavior and sequence of plastic hinge formation are studied for a typical mid-rise building, the 8-45 model.

Elastic Internal Force Distribution

In general, diagonals in diagrid structures undergo large axial forces and comparatively small bending moments under lateral loading, which can be attributed to their inclined position. As such, the axial force is the primary internal force in the design of diagonal members. Figure 3 shows the elastic distribution of axial forces in the diagonals of the 8-45 model due to the earthquake load. In general, axial forces in the diagonals under lateral loading increase from the top story to the first story. Depending on the direction of the lateral load, about half of the diagonals undergo tension and the other half compression. The axial force also increases from the middle diagonals to the corner ones (Figure 3), which indicates the critical role of corner diagonals in diagrids. To take this nonlinear variation of stress between corner and middle members, known as a shear lag effect, one can use smaller sections for middle diagonals. Shear lag is a nonuniform, nonlinear distribution of the internal forces across the side of a tube-shaped structure or structural member. The result is large internal forces in corner members compared with the middle ones.

At each joint, four diagonal members are connected in two different inclined directions (each two are aligned). Corner joints experience either a large compression or a large tension force in one direction/alignment, only while middle joints undergo both compression and tension forces but in smaller magnitudes in two different directions/alignments. As such, this varied load bearing condition of diagrid connections that depends on their locations has a major effect on their connection design. This finding has two implications. First, researchersperforming experiments on connections in diagrids (Kim et al., 2010) need to take the load variation into consideration. Second, the current design preference of fabricators to use as many identical connections as possible needs to be revisited.

Maximum nonfactored diagonal axial forces in the first story due to gravity and earthquake loads are found to be 133 kips and 745 kips, respectively, while the maximum bending moments due to gravity and earthquake loads are relatively small, 14 kip-ft and 67 kip-ft, respectively. Similar differences are noted for diagonals in other stories showing the dominance of axial force in the diagonals compared with bending moment. Consequently, in preliminary design,

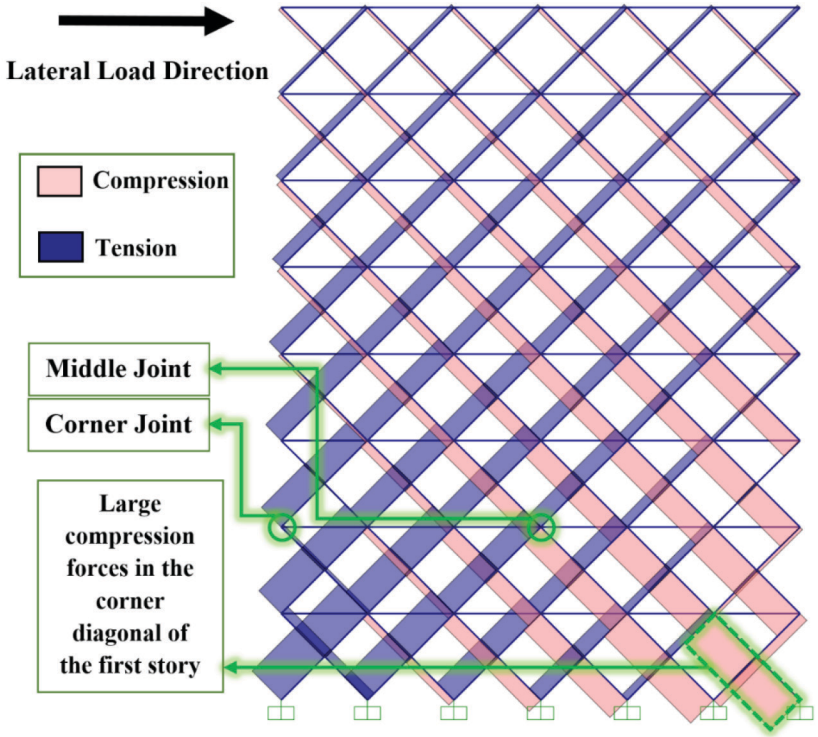

Fig. 3. Axial force in diagonals of 8-45 model due to earthquake load.

Table 1. Modeling Parameters and Acceptance Criteria for Nonlinear Analysis for Diagonal Members of Steel Diagrid Frame Adapted from FEMA-440 (2005) and ASCE/SEI 41-13 (2014)						
	Modeling Parameters			Acceptance Criteria		
Component	a	b	c	IO	LS	CP
W- or I-shaped section	$0.5\Delta_c$	$8\Delta_c$	0.2	$0.5\Delta_c$	$5\Delta_c$	$7\Delta_c$

the diagonals may be designed as axial-force compression members neglecting the small, existing, axial force-bending moment interaction.

The first two vibration modes of the 8-45 diagrid are translational modes with a fundamental period of 0.41 sec obtained using the free vibrations theory and direct eigenvalue method, while the approximate fundamental period equation $T_a = C_t h_n^x$ of ASCE/SEI 7 (2010) yields a larger value of 0.59 sec. This may lead to a nonconservative initial design. Research is needed to create relatively accurate approximate equations for estimating the fundamental period of diagrid structures similar to those developed for MRF (Young and Adeli, 2014a), CBF (Young and Adeli, 2014b), and EBF (Young and Adeli, 2016).

Nonlinear Behavior

In practice, the great majority of structures are designed based on the elastic analysis (Shan et al., 2016; Oh et al., 2017; Kim et al., 2017). During major earthquakes, however, structural members often experience nonlinear inelastic behavior (Adeli et al., 1978; Jiang and Adeli, 2005; Yang et al., 2017). To investigate nonlinear characteristics of diagrids, a static nonlinear analysis is conducted for all models according to the provisions of FEMA-356 (2000) and FEMA-440 (2005) and examples provided in FEMA P-751 (2012). As required by FEMA provisions, lateral loads are applied after the full exertion of gravity loads. They are increased proportionately until a sufficient number of plastic hinges (PH) or fully yielded axial force members result in a failure mechanism. As discussed, diagonals carry mostly axial loads, whereas beams have a large bending moment and columns carry a combination of axial force and bending moment. To model these different types of behavior, three types of PH are defined: axial (P) for diagonals, flexural (M) for beams, and interacting (PMM) for columns (CSI, 2011). The concentrated PH are assigned to mid-length of diagonals, and ends of beams and columns as suggested by FEMA (2000). The scale factors for yield rotation, θ_y, are modeled per Equations 5-1 through 5-4 of FEMA-356 for each PH.

For each member of the structure, three levels of performance are defined as follows: immediate occupancy (IO) after the earthquake, where buildings *"are expected to sustain minimal or no damage to their structural elements and only minor damage to their nonstructural components"*; life safety (LS), where buildings *"may experience extensive damage to structural and nonstructural components"*; and collapse prevention (CP), where buildings *"may pose a significant hazard to life safety resulting from failure of nonstructural components"* as defined in the general force-deformation curve shown in Figure 4 for primary elements (FEMA, 2000, 2005; ASCE, 2014).

To capture the nonlinear behavior of diagonals at each performance level, the recommended modeling parameters and criteria of FEMA-440 and ASCE/SEI 41-13 (2014) for concentrically braced frames, listed in Table 1, are adopted in this investigation. The parameters *a*, *b*, and *c*, shown in Figure 4, are calculated based on FEMA-440, Tables 5-6 and 5-7, and are used for modeling the force-deformation relationship of the PH. The parameter Δ_c represents the axial deformation at the expected buckling load. This method captures global buckling but not local buckling explicitly. Due to large axial forces in the diagonals, a main factor in the load capacity and performance of each diagonal is the cross-sectional area. The required slenderness for the diagonal section is typically low, well below the slender limit between elastic and inelastic buckling ($KL/r = 4.71\sqrt{E/F_y}$ for grade 50 steel). Hence, noncompact sections are intentionally avoided in the design process to limit partial or global buckling while preserving the desirable performance of the system.

In addition, for nonlinear pushover analysis, FEMA-356 provisions require checking at least two different vertical load distributions. In this research, three different vertical load distributions are considered for the entire structure: uniform distribution, the distribution provided by the ELF method of ASCE/SEI 7 (ASCE, 2010), and modal shape distribution considering only the first two modes of vibrations. Out of the three, the most critical pattern is chosen for further study. The center of mass at the roof is used as the monitoring point for the displacement-control pushover analysis. The Newton-Raphson method is used for nonlinear analysis, and the convergence tolerance and maximum number of iterations are adjusted to achieve proper convergence (FEMA, 2000; CSI, 2011).

Figure 5(a) shows the results of the pushover analysis for the 8-45 model. Figure 5(b) shows the lateral stiffness of the structure at the roof level versus the lateral displacement at

the top of the 8-45 model. It is observed that the structure shows the smallest load capacity and the lowest elastic stiffness for the case of mode shape vertical force distribution pattern. Thus, the mode shape distribution is considered the most critical and is selected for further discussion on this model. The same procedure is adopted for other example structures.

The design base shear obtained using the ELF method of ASCE/SEI 7 for 8-45 is approximately 5,845 kips [shown in Figure 5(a) with a dash-dotted line], while at the formation of the first PH [shown in Figure 5(a) with a solid circle], the base shear is 8,318 kips. A part of this 42% overstrength can be attributed to the assumed *R* factor in the design procedure. Figure 5(b) represents the slope of the pushover curve in Figure 5(a). This slope decreases substantially after the formation of the first PH. The structure experiences its ultimate load capacity of 17,310 kips at the CP performance level, which is approximately three times greater than the design base shear.

This diagrid structure remains elastic up to a very low drift ratio of 0.2%, approximately corresponding to the lateral displacement of 2.6 in. in Figure 5(b). From this point on, development of plasticity in the diagonals leads to a sharp decrease in the lateral stiffness in a nearly step-wise fashion after the formation of each PH. This can be recognized in the pushover curve [Figure 5(a)], where the slope of the pushover curve declines gradually until it reaches the ultimate load. As PH are formed or global buckling occurs in several diagonals, the lateral stiffness of the structure is reduced from the yield load [initiation of yielding represented by the horizontal plateau in Figure 5(b)] to the LS performance level, a reduction of 86%. The load capacity of the structure increases up to the ultimate load, beyond which its load capacity drops suddenly, indicating the formation of a failure mechanism. At this point, the structure undergoes a drift ratio of 0.8%, which is, as will be discussed later, much smaller than more ductile structural systems, such as MRF.

Figure 6(a) shows the location of the first PH for each performance level. The first PH of LS level forms in the compression diagonal located at the corner of the first story. This is mostly due to large cumulative axial forces in the corner diagonals. The nonlinear analysis also confirms that corner diagonals undertake the largest amount of axial force compared to other diagonals. In general, diagrid structures consist of a number of diagrid planes on the exterior of the building, and each plane behaves similar to a plate or shell (in the case of curved planes) under lateral loads. In this case, the corner diagonals are at the interface of two diagrid planes and take loads from both. In the case of two perpendicular diagrid frames, one frame, called the flange diagrid frame, is parallel to the direction of lateral force and the other, called the web diagrid plane, is perpendicular to the former. As shown in Figure 3, diagonals in a flange diagrid frame undergo both compression and tension but in the web frame, they are either in compression or tension, depending on the direction of lateral load. Accordingly, the corner diagonals, at the interface of web and flange frames, usually receive large cumulative compression and tension forces from both frames, making them the critical members in diagrids.

When LS PH develop in several compression diagonals, the first IO PH is formed in the corner tension diagonals of the first story (compression members buckle). As the structure is pushed to a larger amount of lateral load, PH spread to other compression diagonals in the first and fourth story. Eventually, plasticity is spread to most diagonal members, and the structure turns into a failure mechanism in the form of a soft story mechanism [fourth story in Figure 6(b)]. At this step of the analysis, plasticity is developed over a good portion of the structure, indicating the ability of a diagrid structure to develop a good number of PH before failure.

In order to explain why more PH form in the fourth story and at a higher performance level than the first three stories, different factors were studied. It was found that grouping of

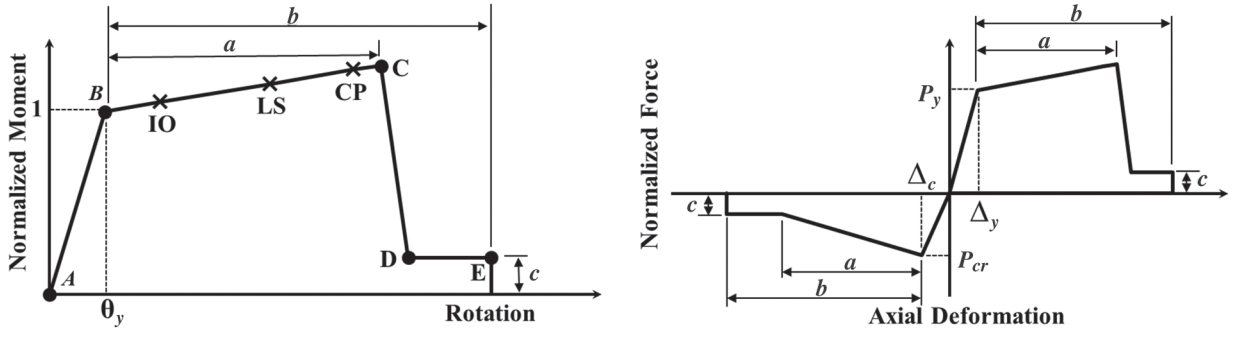

Fig. 4. General member force-deformation relationship and performance levels and parameters adopted from FEMA-440 (2005): (a) flexural elements; (b) diagonals.

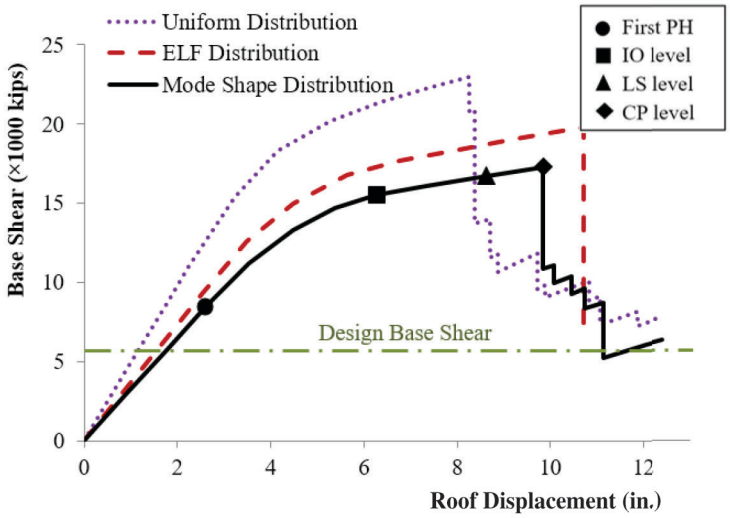

(a)

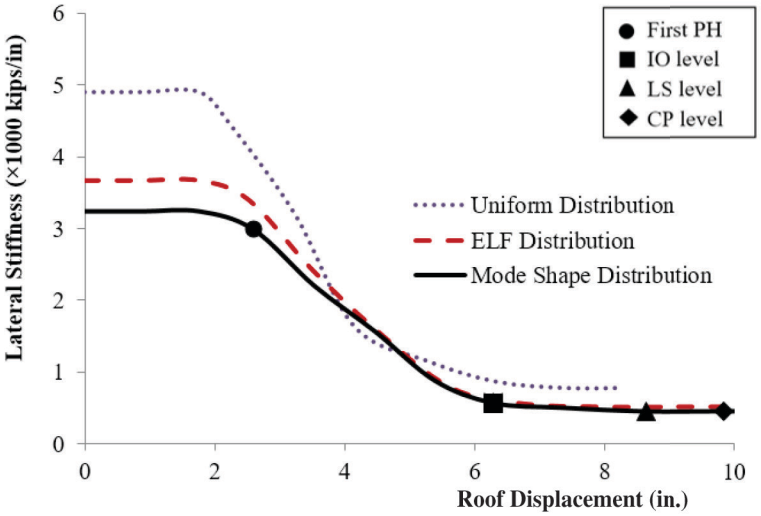

(b)

Fig. 5. (a) Lateral load (pushover) and (b) lateral stiffness versus displacement curve for the 8-45 model.

the members in the design process has the largest influence. Because smaller diagonals are used in the fourth story based on member grouping described earlier, there is a reduction of story stiffness at the fourth story, making it more susceptible to the formation of PH than the story below. It should be noted that ASCE/SEI 7 requirements about irregularity in stiffness or strength were checked and satisfied in the design process.

COMPARISON OF DIAGRIDS WITH MRF AND CBF

General

In this section, the influence of the diagonal angle on the behavior of diagrid structures is studied for 8-story, 15-story, and 30-story models using three different angles of inclination: 45°, 63° and 72°. Further, the 8-story and 15-story diagrid structures are compared with two other commonly used structural systems: MRF and CBF. MRF are well known for their considerable ductility and are chosen to assess the ductility of the diagrids. CBF have inclined members similar to diagrids, but in contrast to diagrids, they also have vertical columns. The plan, elevation loading, and design procedures of MRF and CBF are kept the same as the diagrid. For this comparison, the gravity loads (dead and live load) and the seismic lateral loads are applied to the structure as explained earlier. Figures 7(a) and (b) show the perspective views of the 8-story CBF and MRF models, respectively. In these models, the perimeter diagrid frames are replaced with either MRF or CBF. For CBF, a number of different bracing patterns were examined, and bracing of four bays on each side was found to be the proper choice for carrying the described design lateral loads. The perimeter frames are the primary lateral load-bearing systems in these structures, and central columns absorb only a small portion of the lateral load, similar to the diagrid structures. Table 2 lists the structural properties of the models, including the weight of the structure, fundamental period, maximum story drift, mean story drift, maximum roof displacement, and elastic lateral stiffness at the roof level.

Weight of the Structure

The weight of a steel frame is one of the important factors in choosing an appropriate structural system to carry both vertical and lateral loads. The weight per meter squared for different models is presented in Table 2 and as a bar chart in Figure 8. It is observed that the inclination of the diagonals has a significant impact on the weight of the structure, especially in mid-rise structures in the range of 8 to 15 stories. For the 8-story diagrids, a diagonal angle of inclination of 45° results in the lightest structure. This structure is lighter than the corresponding MRF and CBF by 16% and 7%, respectively. This is primarily due to large columns required in MRF and CBF to carry large lateral loads. The structural efficiency of diagrids may be attributed to their dual function in carrying the gravity and lateral loads. Further, both lateral and gravity loads produce mostly an axial force in the diagonals with little bending moment, which means near-uniform distribution of stresses in the cross-section in contrast to uneven stress distribution in members subjected to bending, a more efficient way to carry a load, as long as

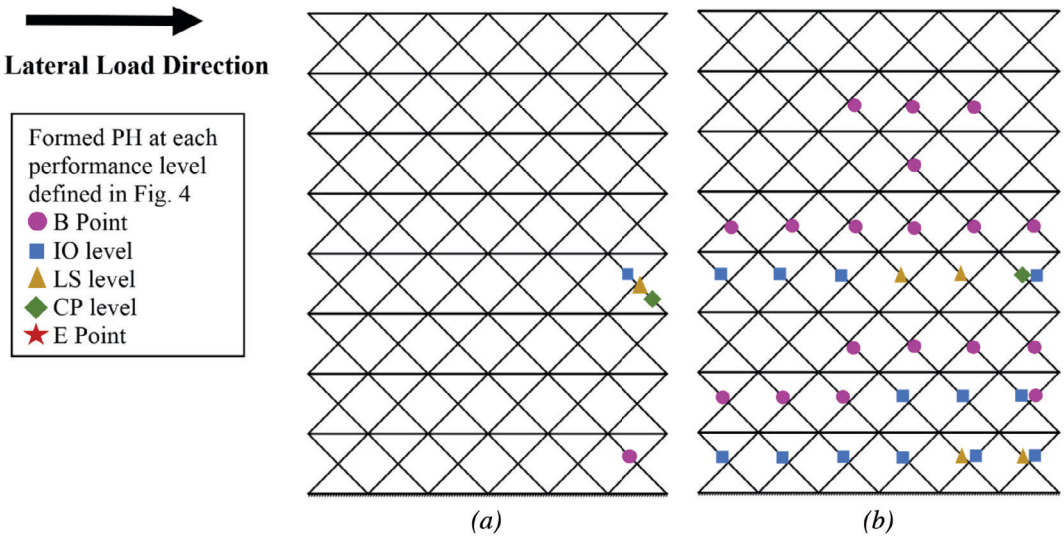

Fig. 6. (a) Location of the first hinge at each performance level; (b) location of PHs at formation of a soft story failure mechanism in the 8-45 structure.

Table 2. Properties of 8-, 15-, and 30-Story Models													
Property	**8-MRF**	**8-CBF**	**15-MRF**	**15-CBF**	**8-45**	**8-63**	**8-72**	**15-45**	**15-63**	**15-72**	**30-45**	**30-63**	**30-72**
Weight of the structure (lb/ft^2)	23.8	21.9	31.2	39.1	20.5	23.2	33.2	33.6	24.4	52.0	44.3	42.2	46.6
Fundamental period (sec)	1.51	0.66	2.50	1.06	0.41	0.37	0.40	0.77	0.73	0.57	1.39	1.26	1.29
Fundamental period using ASCE/SEI 7, $T_a = C_t h_n^x$ (sec)	1.04	0.59	1.72	0.95	0.59	0.59	0.59	0.95	0.95	0.95	1.60	1.60	1.60
Maximum story drift (%)	0.72	0.32	0.75	0.45	0.25	0.21	0.40	0.54	0.46	0.39	0.62	0.29	0.58
Mean story drift (%)	0.65	0.26	0.62	0.37	0.21	0.17	0.23	0.38	0.35	0.24	0.40	0.19	0.33
Maximum roof displacement (in.)	7.16	2.92	12.9	7.63	2.31	1.85	2.50	7.91	7.24	4.86	16.6	7.81	13.6
Elastic lateral stiffness at roof (kip/in.)	409	1748	253	1144	3239	4500	3604	1435	1747	3688	3862	5456	5681

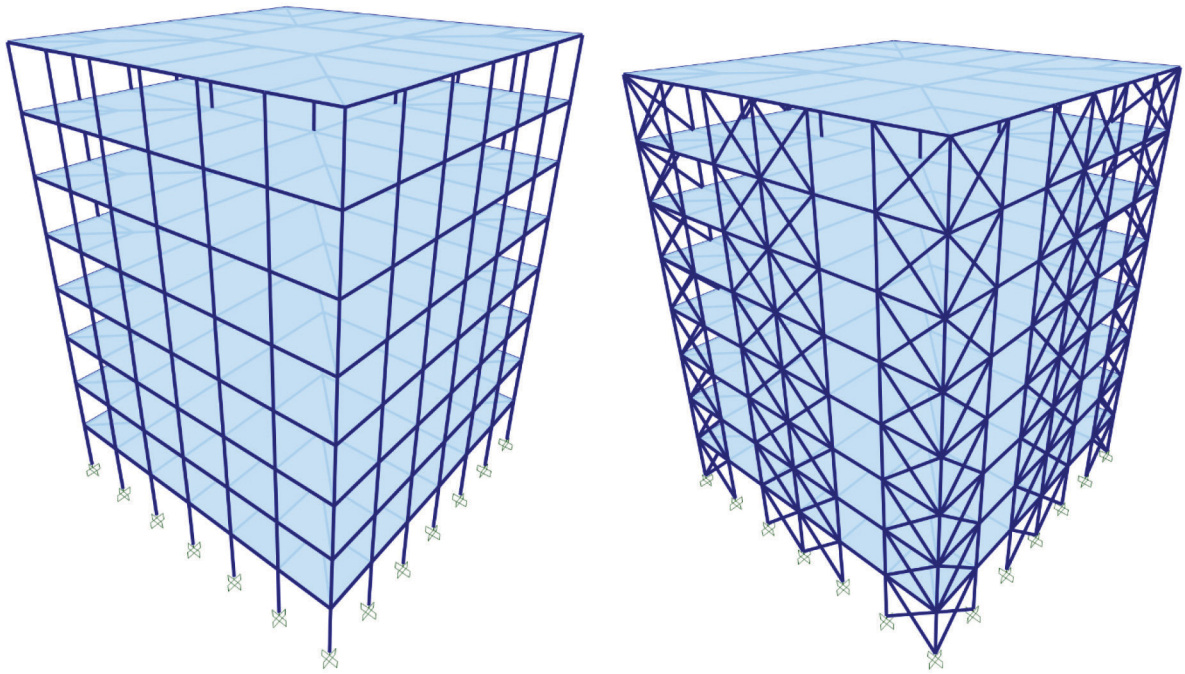

(a) *(b)*

Fig. 7. Perspective view of (a) 8-story MRF; (b) 8-story CBF.

buckling is avoided. As such, it may be concluded that for a mid-rise structure such as the 8-story frames, a diagrid results in a lighter structure compared with MRF and CBF if an appropriate diagonal angle is used. This research complements prior research that pointed to the structural efficiency of diagrids for design of tall buildings in the range of 36 to 100 stories (Moon, 2008; Kim and Lee, 2012).

In the case of the 8-63 and 8-72 models, the diagonal angle has a considerable effect on the total structural weight such that they are 12% and 63% heavier than 8-45, respectively. The following relation exists between the jth lateral load, $F_{L,j}$, and the axial force in the ith diagonal, $F_{d,i}$, neglecting the rest of the structure (Figure 9):

$$F_{L,j} = 2F_{d,i}\cos\theta \tag{3}$$

This equation shows the axial force in the diagonal increases with an increase in the angle θ.

On the other hand, for the 15-story models, the 15-63 model is the lightest and is approximately 20% lighter than 15-45. The 15-63 model is also lighter than both 15-MRF and 15-CBF, indicating a possible reduction of structural weight by using the diagrid structural system. Also, the 15-72 model is substantially heavier than the 15-45 model. The comparative pattern for the 30-story models is similar to 15-story models but on a much smaller scale, where the 30-63 is lighter than the 30-45 and 30-72 models by 4.8% and 10.2%, respectively. The optimal diagonal angle for the minimum weight increases with the height of the structure up to a certain angle, θ. Previous studies reported an optimum diagonal angle in the range of 60° to 70° for 36-story diagrids (Kim and Lee, 2012) and in the range of 65° to 75° for 60-story diagrids having an aspect ratio of about 7 (Moon et al., 2007). The difference in the optimum angle for mid-rise structures, such as the 8-story frames, versus taller structures, such as the 15- and 30-story diagrids, can be explained through the effect of the overturning moment on diagonal axial forces. In taller frames, the overturning moment has a more significant impact on the required strength of diagonal members than the story shear.

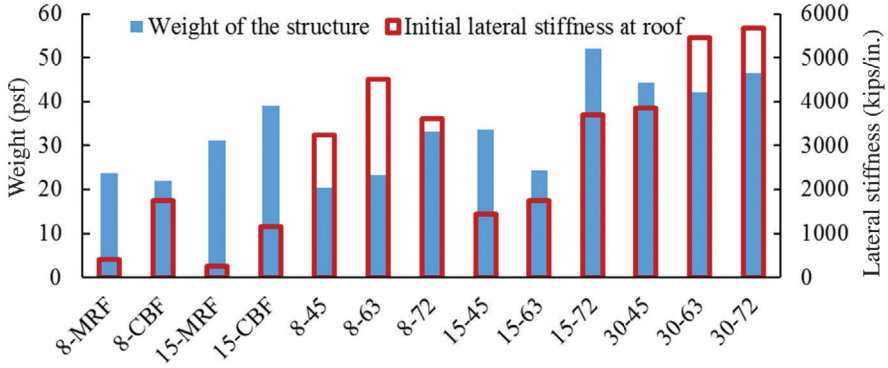

Fig. 8. Comparison of structural weight and lateral stiffness for 8-, 15-, and 30-story models.

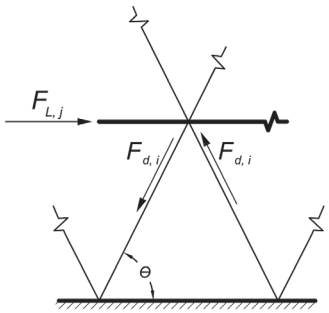

Fig. 9. Relation between the lateral load and axial forces in a pair of diagonals.

Linear Elastic Behavior

Story Drift

Figure 10 shows the variations of story drift along the height of the 8-, 15-, and 30-story models under seismic design base shear. As expected, the MRF shows the largest amount of lateral displacements as well as story drifts among all cases [Table 2 and Figures 10(a) and (b)]. The mean story drift for the MRF is three times larger than that of 8-45 and 2.5 times larger than that of the CBF. In general, diagrid models have lower story drifts than the CBF, as well. In Figure 10(a), two observations are made regarding the CBF. First, the story drift is the largest in the middle stories, which indicates the dominance of shear deformation. Second, the only diagrid with a larger story drift than the CBF is the 8-72 model.

The story drift of the 8-72 model increases considerably at the seventh and eighth stories [Figure 10(a)]. The 72° models consist of a number of 3-story modules along the height of the structure. In case of the 8-72 model, the uppermost module has only two stories (Figure 11), leading to a major increase of the lateral displacement at the seventh and eighth floors. This diagrid pattern is not recommended because it has undesirable elastic as well as nonlinear responses (discussed in the next section).

In diagrids, there are a few jumps in the story drift curve between some neighboring stories, especially in the upper stories of the structure (Figure 10). The jumps are comparatively small in the 45° models but considerably large in the 72° ones. There are two main reasons for this behavior. First, the diagrids are particularly sensitive to the diagonal axial strength, and a small change of diagonal cross-section has a considerable effect on their story drift and elastic response. Second, this behavior is partly due to the way diagonals

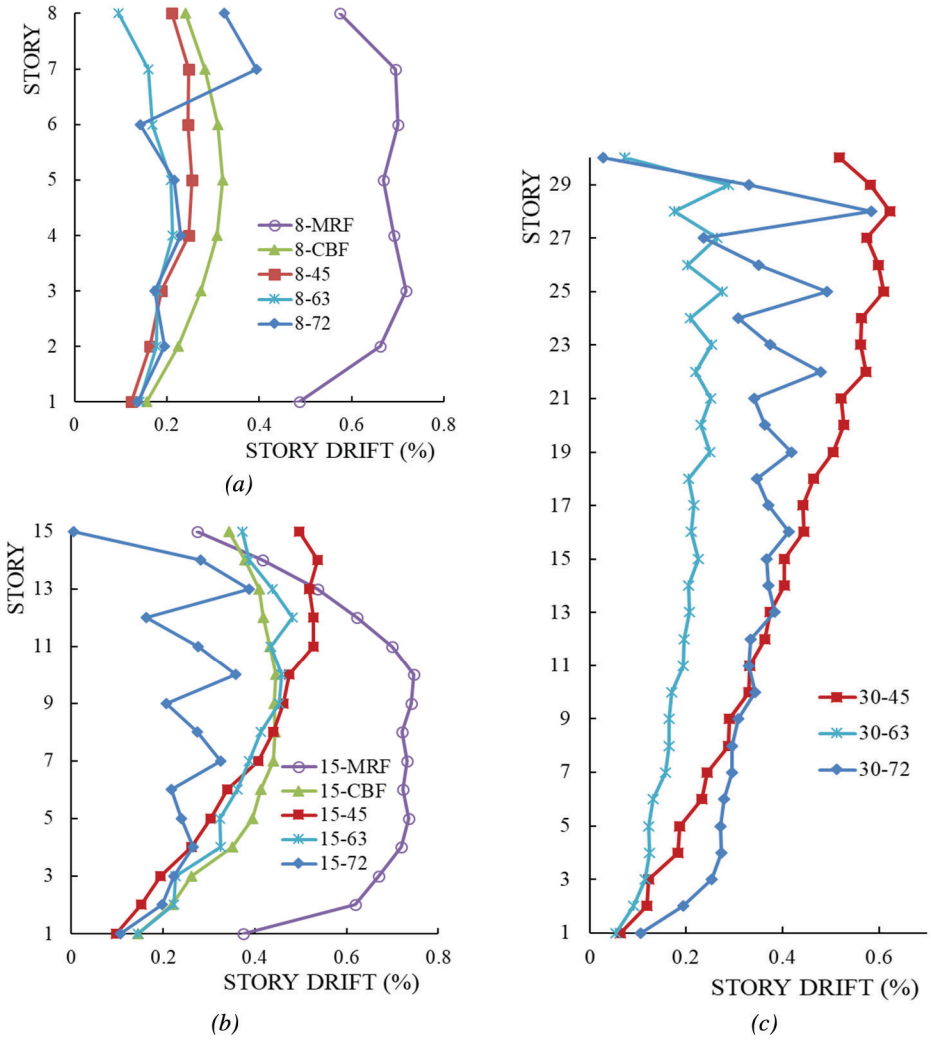

Fig. 10. Comparison of story drift for (a) 8-; (b) 15-; (c) 30-story models.

intersect with the floor beams. In each diagrid module, diagonals may intersect with the floor beams somewhere within the beam span rather than at the beam ends. This adds extra joints to the system, which affects its elastic response. For example, in the 8-72 model, at floors 3 and 6, the diagonals intersect at the beam ends, but at floors 1, 2, 4, 5, 7 and 8, they intersect somewhere within the floor beam span (Figure 11). This particular connection arrangement has a major effect on the nonlinear response of the system as well (discussed in the next section).

Lateral displacement changes similarly along the height of the 15- and 30-story models. As shown in Figures 10(b) and (c), story drift curves of the 15- and 30-story diagrids have also a number of noticeable sudden changes along the height. In the 15-story models, the 15-72 model has the smallest mean story drift but with more noticeable jumps at every three stories (where the diagonal cross-section changes). The mean story drifts for 15-45, 15-63 and 15-CBF are relatively close (Table 2). Among the 30-story models, however, the 30-63 has the smallest mean story drift similar to the 8-story models. The story drift of the 30-72 model is the largest for the lower one-third part of the structure but becomes smaller than that of 30-45 model from the 11th story to the roof. Therefore, the effect of the diagonal angle on lateral stiffness is not uniform along the height and may vary from story to story.

Fundamental Period

The mean fundamental period of diagrid models is less than the fundamental period of the MRF and CBF models (Table 2). The fundamental period of diagrids is also smaller than the generally conservative approximate period equation provided by ASCE/SEI 7 (2010), $T_a = C_t h_n^x$, by up to 59%. This indicates a need to develop more accurate approximate equations for diagrids as explained earlier.

Elastic Lateral Stiffness

Figures 12(a), (c), and (d) show the pushover curves for the 8-, 15-, and 30-story models, respectively. Figure 12(b) shows the lateral displacement curves for the 8-story models. The pushover curves start with a constant slope representing the elastic lateral stiffness reported in Table 2. As indicated in Table 2, mean initial stiffness of the 8-story diagrids is considerably larger than those of 8-MRF and 8-CBF models, by 90% and 54%, respectively. Similarly, the mean initial stiffness of the 15-story diagrids is 89% and 50% larger than 15-MRF and 15-CBF, respectively.

Figure 8 illustrates a comparison of the elastic stiffness of different models. Among 8-story diagrids, 8-63 has the largest lateral stiffness and load carrying capacity [Figures 12(a) and (b)]. This is partly due to its near-optimal diagonal angle under a combination of shear load and overturning moment.

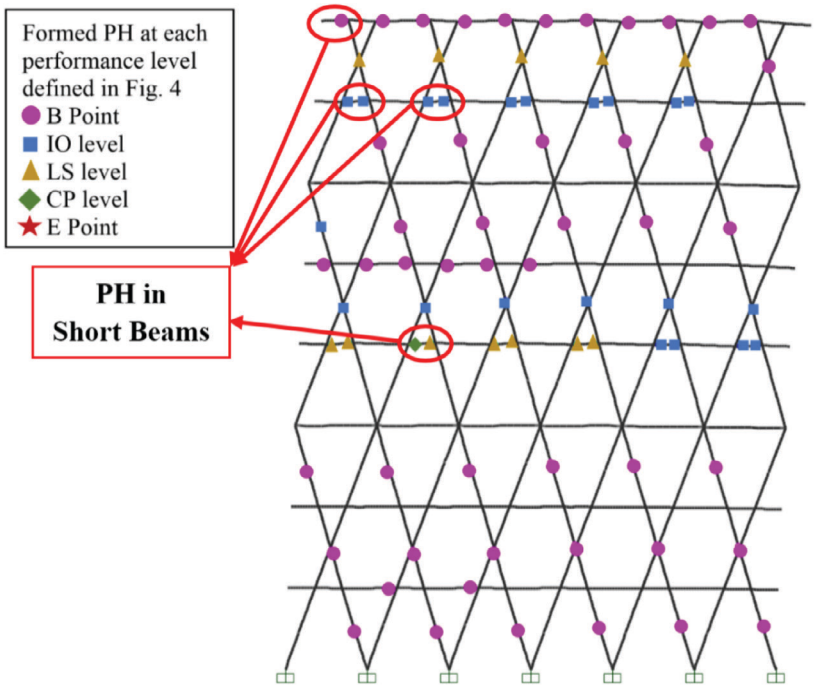

Fig. 11. Deformed shape of 8-72 model at the ultimate load magnified by a factor of 6.

The 8-72 model also shows a larger lateral stiffness than the 8-45 model, despite the fact that the uppermost module of diagrid in the 8-72 model is an incomplete 2-story module. This indicates that the 72° of the diagonal angle may result in better behavior in terms of lateral stiffness. This observation is confirmed in the 15-story models, where the 15-72 model has the largest elastic lateral stiffness [Table 2 and Figure 12(c)].

Sequence of Plastic Hinge Formation and Failure Mechanism

Plastic analysis and study of the formation of PH provide insight into the nonlinear behavior of structures (Adeli and Chyou, 1986). This section is a comparative study of the nonlinear plastic behavior of all models under lateral pushover load. The assumptions for this section are the same as those given earlier. The sequence of PH formation in the diagonals generally depends on these factors: the axial demand-to-capacity ratio of the diagonals (the reciprocal of the member overstrength factor), the diagonal location in the plan and elevation, and the type of stress in the diagonals (compressive or tensile). PH will start developing in the diagonals with a larger axial demand to capacity ratio (near the ratio of 1.00) first. Furthermore, because of buckling and shear lag, the farther the diagonal is from the compressive corners, the later the formation of the PH will be. Due to the shear lag effect, corner diagonals are more likely to form PH first than other diagonals of each story. In addition, depending on the direction of the lateral load, the diagonals under compression are likely to fail earlier than those under tension.

The first PH in all diagrid models is formed in the diagonal located at the corner of the first story. Figure 11 shows the deformed shape of the 8-72 model at its ultimate load magnified by a factor of 6. PH developed at the start of the inelastic behavior (point B in Figure 4); performance levels

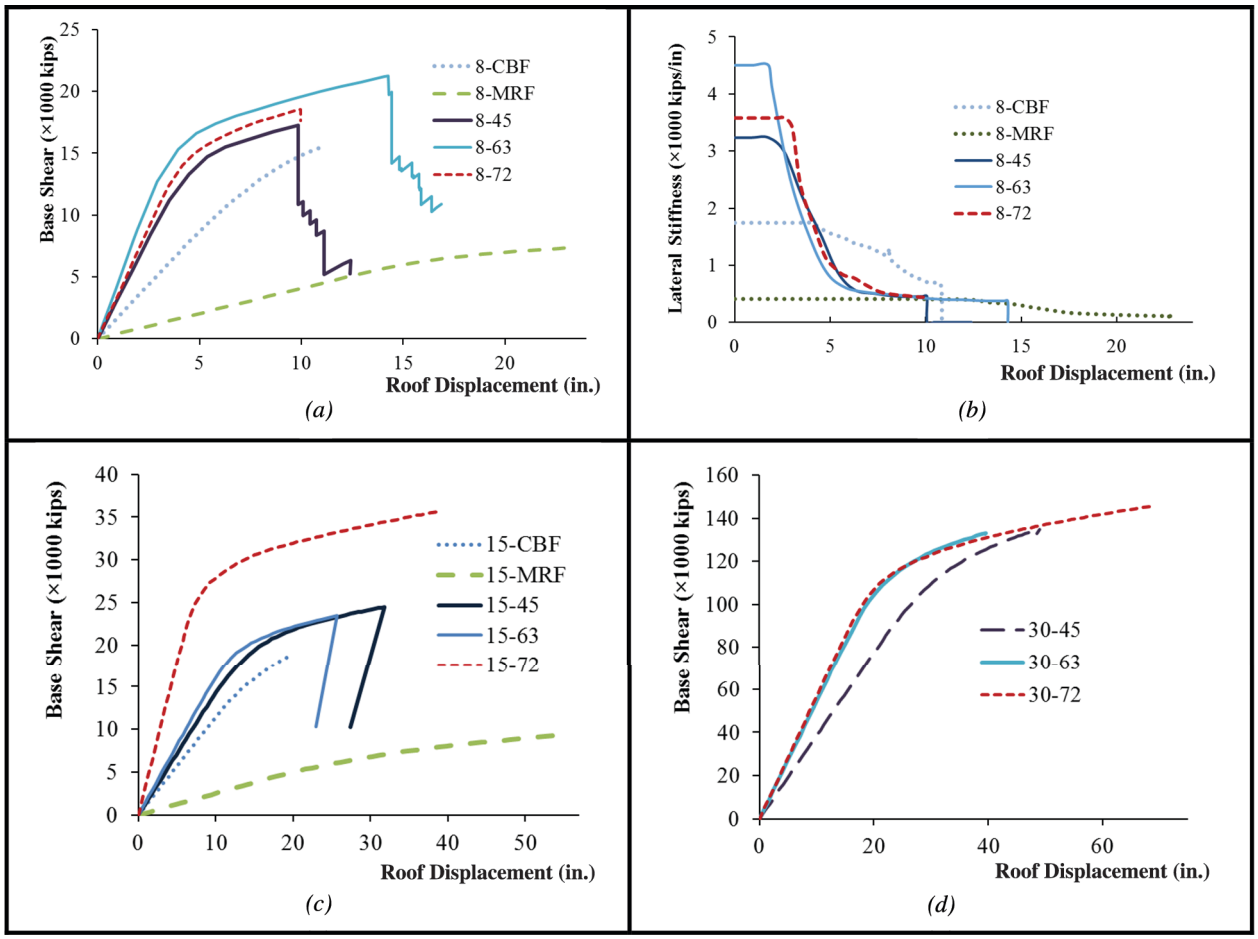

Fig. 12. (a) Pushover curves for 8-story models; (b) lateral stiffness curves for 8-story models; (c) pushover curves for 15-story models; (d) pushover curves for 30-story models.

IO, LS and CP; and the rupture point (point E in Figure 4) are identified by solid circles, squares, triangles, diamonds and stars, respectively. Diagrids having a 72° diagonal angle show a different behavior than the 45° and 63° models in terms of PH formation. In 72° models, PH spread to floor beams early and develop relatively quickly one after another compared to the 45° and 63° models. This distinctive behavior is related to the way diagonals intersect within the span of the floor beams in these models, as explained earlier, which creates a series of short floor beams. These short beams shown in Figure 11 are where the early PH are formed. Depending on the diagonal angle, story height, and floor plans, such connections are likely to be used in diagrids, and their distinctive inelastic behavior need to be addressed properly in the frame and the connection design procedure.

The 8-63 structure shows a better plastic behavior than the 8-45 and the 8-72 ones. In the 8-63 structure, hinges are spread both horizontally and vertically across the structure more broadly than the other 8-story diagrids. This can be inferred in the pushover curve as the 8-63 model shows a larger load-carrying capacity compared with other models [Figure 12(a)]. In 15- and 30-story models, however, the 72° models show a better distribution of PH across the diagonals and the beams. Figure 13 shows the deformed shape of the 30-72 and 30-45 models at their ultimate load magnified by a factor of 6. This figure shows a large number of PH formed in beams and diagonals of 30-72 model, indicating desirable nonlinear performance and progressively failure, and some of the beam PH are developed at a higher performance level than the diagonal PH.

The governing failure mechanism in the 45- and 63-diagrids studied in this research was found to be a soft-story mechanism. As an example, Figure 14 shows the deformed shape of the 15-63 model at the formation of a soft-story mechanism at the fourth story magnified by a factor of 6. As illustrated, the failure occurs as PH are formed in all compression diagonals, some tension ones, and most floor beams of the fourth story, which is an intermediate story as opposed to the more commonly observed first story. At this point, load-carrying capacity decreases substantially when diagonals reach their rupture limit (point E in Figure 4). Figure 14 depicts a possible undesirable failure

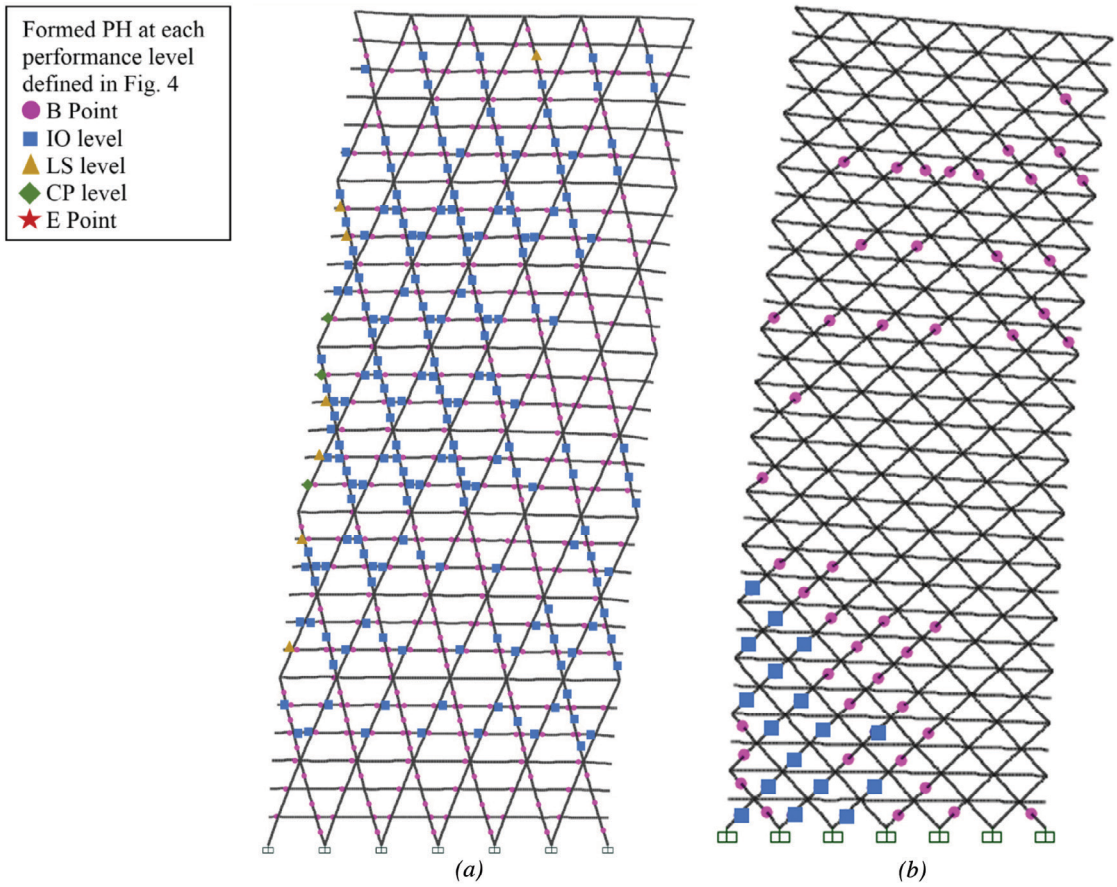

Fig. 13. The deformed shape of the (a) 30-72 and (b) 30-45 models at the ultimate load magnified by a factor of 6.

mechanism in diagrid structures where plastic hinges are not developed properly and premature soft-story failure leads to an overall collapse of the structural system.

PH are well spread across the frame for most cases, except for the 8-72 model (Figure 11). In all cases, the soft story tends to form in an intermediate story of the structure where a major change in diagonal cross-section exists. For instance, the soft story is formed in the fourth and the seventh stories of the 8-63 and the 15-45 models, respectively.

The first few PH in the 8-CBF model are formed in the coupling beams of the fifth floor. This is followed by the formation of PH in the coupling beams of the fourth and sixth floors and the braces of the second and third stories. The first PH in the columns was observed in the compression column of the first story and after formation of several PHs in beams and braces. This sequence is generally desirable because columns should be the last to yield or buckle. In addition, the PH spread to different members across the structure reasonably well. This is basically the sequence of PH formation at different performance levels (IO, LS and CP) for all CBF. The sequence of PH formations for the 15-CBF model is generally similar to 8-CBF, except for the location of the first hinge, which is formed in the fourth-story brace.

In case of MRF, the first PH forms in the compression column of the first story. PH spread to beams and columns of the other stories from lower stories to the roofs and the failure mechanism forms as all columns of the first story form a PH at the top and the bottom ends (first soft-story sway mechanism).

DESIGN CONSIDERATIONS

Virtual Work/Energy Diagram

The concept of virtual work/energy (Cha and Buyukozturk, 2015) and the corresponding distribution diagram can be used effectively to find the members that need to be stiffened to achieve improved structural deformation (CSI, 2011). The virtual work is defined for each degree of freedom (DOF) of the finite element model as the force times the displacement at that DOF. The summation of these virtual works for any member is the virtual work of that member. Figures 15(a) and 15(b) show the normalized virtual work distribution of the diagonals for the 8-45 and 30-72 models along with their height under lateral seismic load, respectively. For the 30-72 model, the mean virtual work of each 3-story module (instead of each story) is illustrated. Moreover, Figure 16 illustrates this distribution for the 8-45 model in a 3D surface diagram. For the sake of comparison, the virtual work values in Figures 15 and 16 are normalized by the maximum virtual work in the structure.

For the web diagrid of the 8-45 model, the corner diagonals

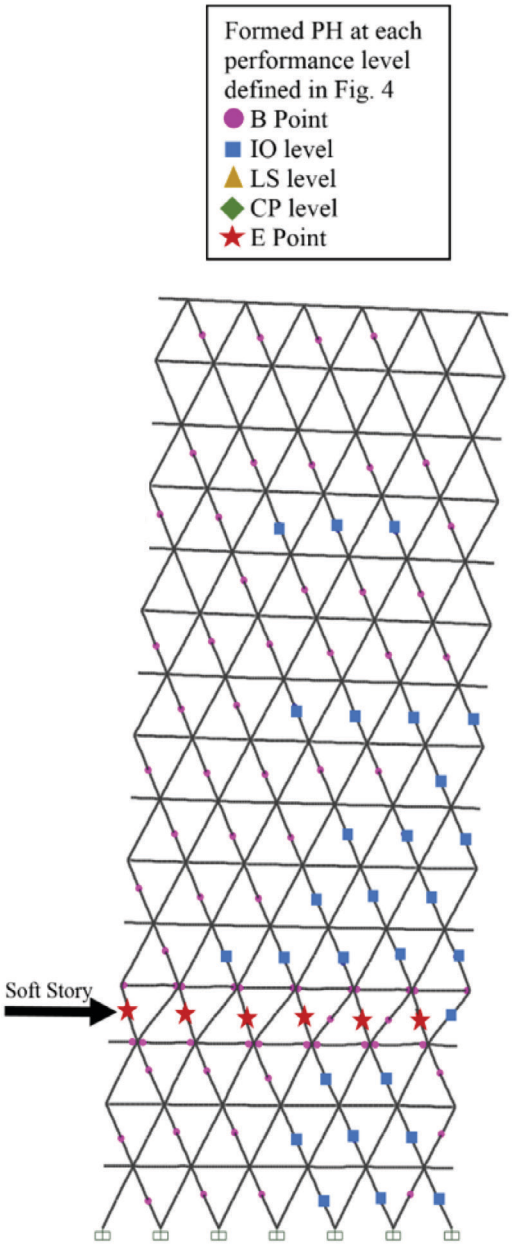

Fig. 14. The deformed shape of the 15-63 model at the formation of a soft-story mechanism at the fourth story magnified by a factor of 6.

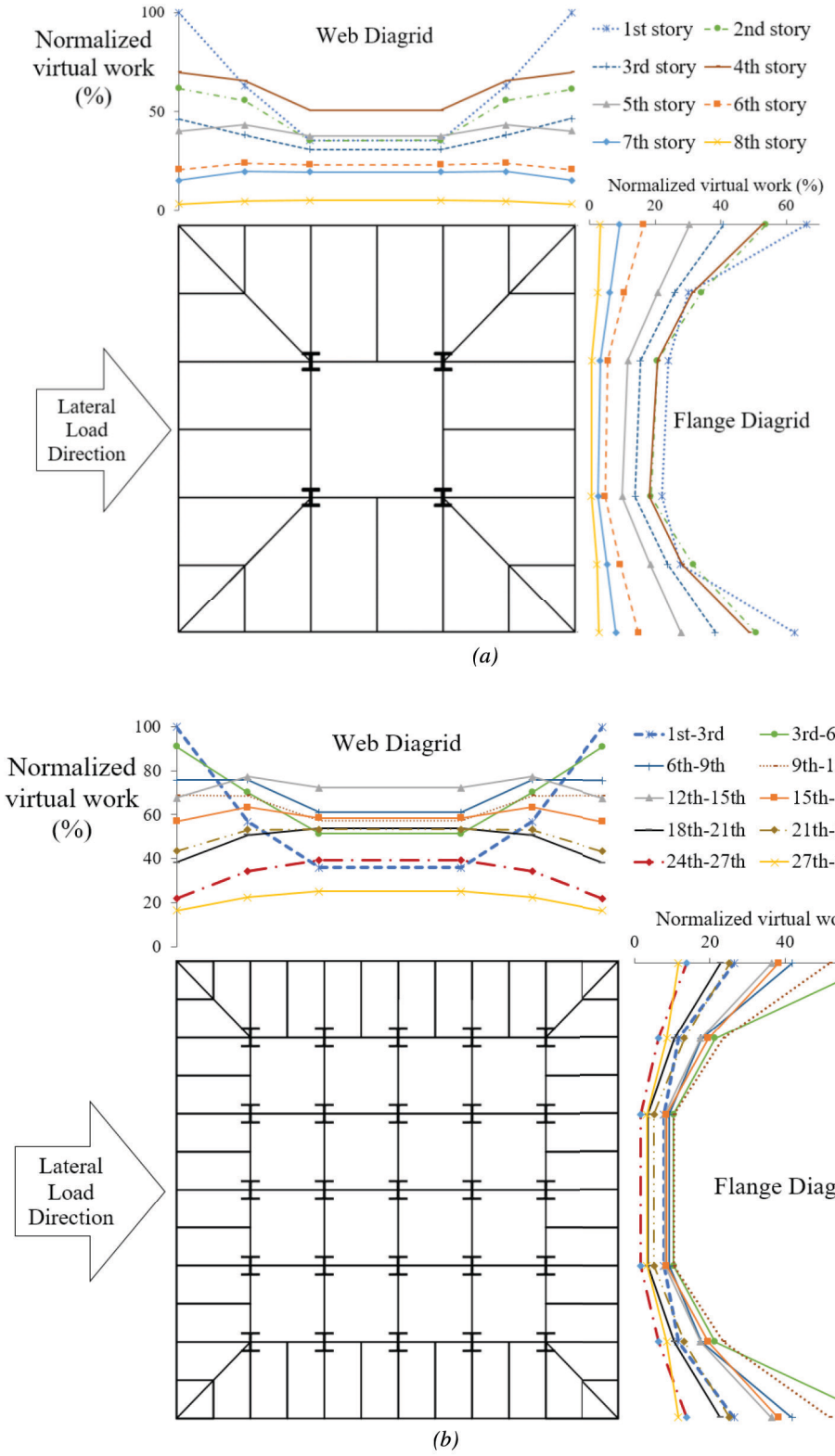

Fig. 15. Normalized virtual work distribution of (a) the 8-45 model for different stories; (b) the 30-72 model for different 3-story modules.

of the first story have the largest virtual work. Other diagonals of the first story have a substantially smaller value. This variation is different for other stories. In the second and the third stories, the difference between the corner diagonals and middle ones is much smaller than that of the first story. Along the height of the structure from the first story to the roof, the virtual work of the corner diagonals decreases while that of the middle diagonals increases. The mean virtual work is reduced from the first to the third stories. But in the fourth story, a sudden increase happens and the virtual work values increase such that they are larger than those of the second and third stories. This is manifested as a peak at the fourth story on the 3D virtual work diagram of the 8-45 model (Figure 16). The fourth story is where the diagonal sections are reduced based on the grouping approach explained earlier. More importantly, the fourth story is where the soft-story mechanism is formed, resulting in the collapse of the structure. The soft story tends to form in the middle one-third section of the structure (approximately between the third and fifth stories) where the mean virtual work is relatively large and the virtual work distribution is near-uniform across the diagrid width. On the other hand, in the one-third uppermost part of the 8-45 diagrid (sixth to eighth stories), the virtual work of the middle diagonals is slightly larger than that of corner ones [Figure 15(a)]. This suggests that in this part of the structure, the middle diagonals need to be stiffer than the corner ones, which is completely dissimilar to the variation observed in the lower stories (first to fifth). In addition, the mean amount of virtual work in the upper stories (sixth to eighth) is considerably smaller than that of the lower ones, indicating that the upper stories are not critical in terms of lateral displacement.

In the flange diagrid, the virtual work variation for different stories is similar [Figure 15(a)]. The virtual work is larger in the corner diagonals for all stories and, similar to the web diagrid, there is some noticeable increase in the virtual work of the fourth story. Nonetheless, the mean value for the flange diagrid is smaller than that of the web diagrid.

Other models, including the 30-72, have a similar distribution of virtual work across the height and width of the web and flange diagrids. In the case of the 30-72 model [Figure 15(b)], the corner diagonals of the first module have the largest virtual work, whereas the middle diagonals of that module have a significantly smaller virtual work. From the 18th story to the 30th (approximately uppermost one-third of the structure), this variation is inverted, and the middle diagonals have a larger virtual work than the corner ones. Furthermore, the jumps due to the change of the diagonal section are not quite noticeable because diagonal sections are changed in each module every three stories.

General Recommendations

Under lateral loads, diagrids behave predominantly analogous to thin plates, where the diagonal grids form a thin plate subjected to in-plane lateral loads. This similarity is useful in developing practical design methods and formulas for diagrid design. The lateral displacement of diagrids is mostly due to overall bending of the structure known as chord drift as opposed to the shear lateral deformation,

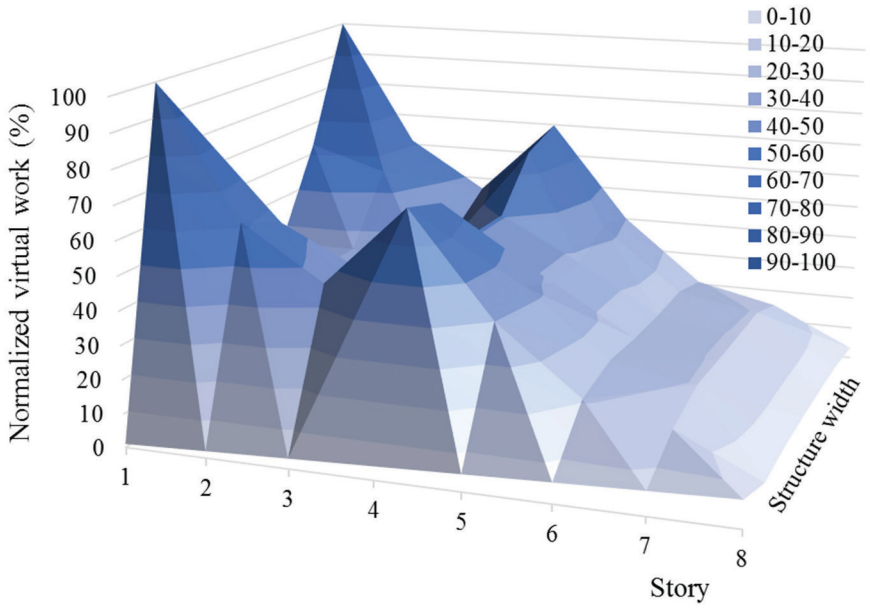

Fig. 16. Normalized virtual work distribution for different stories in the web diagrid of the 8-45 model.

similar to the bending deformation of shear walls. In a bending displacement, corner members in the web loading plane are under large compression or tension in all stories, and these forces are particularly large in the lowest stories.

According to the virtual work diagrams, the shear lag effect is more significant in the first module of the diagrid, usually the first story. The corner diagonals of these stories are always the critical member of the structure, and their virtual work is significantly larger than other members. According to nonlinear analysis, these diagonals are the first to yield and, accordingly, the key member in overall load-carrying capacity of the structure. Thus, special design considerations, such as a larger overstrength factor for these members, can prevent premature failure and increase the ultimate load capacity of the structure.

Diagonal axial strength has a major influence on the diagrid behavior and failure mechanism. To prevent an early soft-story mechanism, the size of the diagonal cross-section should be changed gradually as much as possible. Using different diagonal sections across the width of the frame in addition to the grouping across the height can improve the structural efficiency significantly and, if carefully considered, can prevent the undesirable soft-story failure mechanism under extreme loadings. In this regard, compared with other structural systems, a key difference is the shear lag effect in diagrids—in other words, the significance of corner diagonal members. The ASCE/SEI 7 (2010) criteria for soft- and weak-story consider the stiffness of the whole story and do not necessarily prevent the soft-story mechanism initiated in corner diagonals. In high seismic regions, a synthesis of these recommendations can improve the linear and nonlinear response of the diagrid system and, possibly, its ductility.

CONCLUSIONS

This research demonstrated that diagrid can be a practical and efficient structural system in mid- to high-rise buildings. Using diagrids with an appropriate diagonal angle, the designer can significantly reduce the weight of the structure as well as the mean story drift of the building. In general, diagrids in the 8- to 15-story range have a smaller mean story drift than CBF and MRF, except for the 15-45 model, whose mean story drift is 4% larger than the 15-CBF model.

In general, due to the shear lag effect, the corner diagonals are under a larger amount of internal forces than the other diagonals of the same story. However, according to the virtual work diagrams, this difference is reversed in approximately the uppermost one-third of the structure, where the middle diagonals have a larger amount of virtual work and, consequently, are more critical than other members of that story. The axial force is the major internal force in diagonals, and preliminary design of diagrids based on axial force is a reasonable assumption.

The ASCE/SEI 7 equation for finding the approximate fundamental period ($T_a = C_t h_n^x$,) yields a generally nonconservative result for diagrids because their fundamental period is notably smaller than that of CBF and MRF. Current codes of design also offer no specific value for diagrid ductility, overstrength, and response modification factors, and using the smallest values for those factors is largely conservative for diagrids.

Diagrids have a considerably larger initial stiffness (in the elastic region) compared to MRF and CBF, and likewise, CBF have a larger lateral stiffness compared to MRF. In terms of nonlinear behavior, diagrids show smaller ductility compared with the MRF. Lateral stiffness of diagrids decreases relatively sharply as the PH are formed in the diagonals, and they reach their corresponding ultimate load at a smaller lateral displacement than the MRF. Ductility is a highly desirable property in high seismic regions for dissipating the earthquake energy. Thus, in high seismic regions, low ductility of diagrids is an issue that should be addressed. To resolve this issue, a solution would be addition of passive dampers (such as viscoelastic dampers) (El-Khoury and Adeli, 2013; Fisco and Adeli, 2011b; Gutierrez-Soto and Adeli, 2013a) or semi-active control systems (such as semi-active hydraulic dampers) (Fisco and Adeli, 2011a; Gutierrez-Soto and Adeli, 2013b) along the diagonals of diagrids. Inclined corner members of the diagrid are the most appropriate locations for installing passive or semi-active control systems to improve the overall ductility of the structure.

Diagrids are particularly sensitive to the diagonal axial strength and sudden changes of diagonal cross-section across the height and the width of the structure should be avoided because it may result in a soft-story mechanism. The soft story tends to form in the middle one-third of the structure, where the virtual work distribution is near uniform across the diagrid width.

In recent years, significant research has been reported on design optimization of high-rise building structures using nature-inspired computing techniques such as the genetic algorithm (Adeli and Sarma, 2006; Mencia et al., 2016) and the patented neural dynamics model of Adeli and Park (Adeli and Park, 1998). Applications of formal optimization techniques to high-rise diagrid structures can result in additional structural efficiencies which are currently being pursued by the authors. Other technologies yet to be applied to diagrid structures are semi-active and active vibration control (Yeganeh-Fallah and Taghikhany, 2016; Karami and Akbarabadi, 2016) and structural health monitoring (Lin et al., 2017; Tsogka et al., 2017; Cha et al., 2017).

REFERENCES

Adeli, H. and Chyou, H. (1986), "Plastic Analysis of Irregular Frames on Microcomputers," *Computers and Structures*, Vol. 23, No. 2, pp. 233–240.

Adeli, H., Gere, J. and Weaver, W.J. (1978), "Algorithms for Nonlinear Structural Dynamics," *Journal of Structural Division,* ASCE, Vol. 104, No. 2, pp. 263–280.

Adeli, H. and Park, H.S. (1998), *Neurocomputing for Design Automation*, CRC Press, Boca Raton, FL.

Adeli, H. and Sarma, K. (2006), *Cost Optimization of Structures—Fuzzy Logic, Genetic Algorithms, and Parallel Computing*, John Wiley and Sons, West Sussex, United Kingdom.

AISC (2011), *Steel Construction Manual,* 14th Ed., American Institute of Steel Construction, Chicago, IL.

AISC (2016a), *Seismic Provisions for Structural Steel Buildings*, ANSI/AISC 341-16, American Institute of Steel Construction, Chicago, IL.

AISC (2016b), *Specification for Structural Steel Buildings*, ANSI/AISC 360-16, American Institute of Steel Construction, Chicago, IL.

Ali, M.M. and Moon, K.S. (2007), "Structural Developments in Tall Buildings: Current Trends and Future Prospects," *Architectural Science Review*, Vol. 50, No. 3, pp. 205–223.

Asadi, E. and Adeli, H. (2017), "Diagrid: An Innovative, Sustainable and Efficient Structural System," *The Structural Design of Tall and Special Buildings*, Vol. 26, No. 8 (11 pages).

ASCE (2010), *Minimum Design Loads for Buildings and Other Structures*, ASCE Standard ASCE/SEI 7, American Society of Civil Engineers, Reston, VA.

ASCE (2014), *Seismic Evaluation and Retrofit of Existing Buildings*, ASCE/SEI 41-13, American Society of Civil Engineers, Reston, VA.

Boake T.M. (2014), *Diagrid Structures: Systems, Connections, Details*, Birkhäuser, Switzerland, http://alltitles.ebrary.com/Doc?id=10838294.

Cha, Y.J. and Buyukozturk, O. (2015), "Structural Damage Detection Using Modal Strain Energy and Hybrid Multi-Objective Optimization," *Computer-Aided Civil and Infrastructure Engineering*, Vol. 30, No. 5, pp. 347–358.

Cha, Y.J., Choi, W. and Buyukozturk, O. (2017), "Deep Learning-Based Crack Damage Detection Using Convolutional Neural Networks," *Computer-Aided Civil and Infrastructure Engineering*, Vol. 32, No. 5, pp. 361–378.

CSI (2011), *CSI Analysis Reference Manual for SAP2000, ETABS, SAFE, and CSiBridge*, Computers and Structures Inc., Berkeley, CA.

El-Khoury, O. and Adeli, H. (2013), "Recent Advances on Vibration Control of Structures under Dynamic Loading," *Archives of Computational Methods in Engineering*, Vol. 20, No. 4, pp. 353–360.

FEMA (2000), *Prestandard and Commentary for the Seismic Rehabilitation of Buildings*, FEMA-356, Building Seismic Safety Council for the Federal Emergency Management Agency, Washington, DC.

FEMA (2005), *Improvement of Nonlinear Static Seismic Analysis Procedures*, FEMA-440, Building Seismic Safety Council for the Federal Emergency Management Agency, Washington, DC.

FEMA (2012), *2009 NEHRP Recommended Seismic Provisions: Design Examples*, FEMA P-751, Building Seismic Safety Council for the Federal Emergency Management Agency, Washington, DC.

Fisco, N.R. and Adeli, H. (2011a), "Smart Structures: Part I—Active and Semi-Active Control," *Scientia Iranica*, Vol. 18, No. 3, pp. 275–284.

Fisco N.R. and Adeli, H. (2011b), "Smart Structures: Part II—Hybrid Control Systems and Control Strategies," *Scientia Iranica—Transaction A: Civil Engineering*, Vol. 18, No. 3, pp. 285–295.

Grigorian, M. and Kashani, K.A. (1976), "Plastic Design of Uniformly Loaded Rectangular Diagonal Grids on Simple Supports," *Building and Environment*, Vol. 11, No. 2, pp. 131–138.

Gutierrez-Soto, M. and Adeli, H. (2013a), "Tuned Mass Dampers," *Archives of Computational Methods in Engineering*, Vol. 20, No. 4, pp. 419–431.

Gutierrez-Soto, M. and Adeli, H. (2013b), "Placement of Control Devices for Passive, Semi-active, and Active, Vibration Control of Structures," *Scientia Iranica—Transaction A: Civil Engineering*, Vol. 20, No. 6, pp. 1,567–1,578.

Jiang, X. and Adeli, H. (2005), "Dynamic Wavelet Neural Network for Nonlinear Identification of Highrise Buildings," *Computer-Aided Civil and Infrastructure Engineering*, Vol. 20, No. 5, pp. 316–330.

Karami, K. and Akbarabadi, S. (2016), "Developing a Smart Structure Using Integrated Subspace-Based Damage Detection and Semi-Active Control," *Computer-Aided Civil and Infrastructure Engineering*, Vol. 31, No. 11, pp. 887–902.

Kim, Y., Jung, I., Ju, Y., Park, S. and Kim, S. (2010), "Cyclic Behavior of Diagrid Nodes with H-Section Braces," *Journal of Structural Engineering*, Vol. 136, No. 9, pp. 1,111–1,122.

Kim, J. and Kong, J. (2013), "Progressive Collapse Behavior of Rotor-Type Diagrid Buildings," *The Structural Design of Tall and Special Buildings*, Vol. 22, No. 16, pp. 1,199–1,214.

Kim, J. and Lee, Y.H. (2010), "Progressive Collapse Resisting Capacity of Tube-Type Structures," *The Structural Design of Tall and Special Buildings*, Vol. 19, pp. 761–777.

Kim, J. and Lee, Y.H. (2012), "Seismic Performance Evaluation of Diagrid System Buildings," *The Structural Design of Tall and Special Buildings*, Vol. 21, No. 10, pp. 736–749.

Kim, D., Oh, B.K., Park, H.S., Shim, H.B. and Kim, J. (2017), "Modal Identification for High-Rise Building Structures Using Orthogonality of Filtered Response Vectors," *Computer-Aided Civil and Infrastructure Engineering*, Vol. 32, No. 12, pp. 1,064–1,084.

Lin, Y.Z., Nie, Z.H. and Ma, H.W. (2017), "Structural Damage Detection with Automatic Feature-Extraction through Deep Learning," *Computer-Aided Civil and Infrastructure Engineering*, Vol. 32, No, 12, pp. 1,025–1,046.

Mencıa, R., Sierra, M.R., Mencıa, C. and Varela, R. (2016), "Genetic Algorithms for the Scheduling Problem with Arbitrary Precedence Relations and Skilled Operators," *Integrated Computer-Aided Engineering*, Vol. 23, No. 3, pp. 269–285.

Moon, K.S. (2008), "Sustainable Structural Engineering Strategies for Tall Buildings," *The Structural Design of Tall and Special Buildings*, Vol. 17, No. 5, pp. 895–914.

Moon, K.S., Connor, J.J. and Fernandez, J.E. (2007), "Diagrid Structural Systems for Tall Buildings: Characteristics and Methodology for Preliminary Design," *The Structural Design of Tall and Special Buildings*, Vol. 16, No. 2, pp. 205–230.

Oh, B.K., Kim, D. and Park, H.S. (2017), "Modal Response-Based Visual System Identification and Model Updating Methods for Building Structures," *Computer-Aided Civil and Infrastructure Engineering*, Vol. 32, No. 1, pp. 34–56.

Rafiei, M.H. and Adeli, H. (2016), "Sustainability in High-rise Building Design and Construction," *The Structural Design of Tall and Special Buildings*, Vol. 25, No. 13, pp. 643–658.

Shan, J., Ouyang, Y., Yuan, H.W. and Shi, W. (2016), "Seismic Data Driven Identification of Linear Physical Models for Building Structures Using Performance and Stabilizing Objectives," *Computer-Aided Civil and Infrastructure Engineering*, Vol. 31, No. 11, pp. 846–870.

Subramanian, G. and Subramanian, N. (1970), "Analysis of Simply Supported Uniform Diagrids," *Building Science*, Vol. 4, No. 4, pp. 209–215.

Tsogka, C., Daskalakis, E., Comanducci, G. and Ubertini, F. (2017), "The Stretching Method for Vibration-Based Structural Health Monitoring of Civil Structures," *Computer-Aided Civil and Infrastructure Engineering*, Vol. 32, No. 4, pp. 288–303.

Wang, N. and Adeli, H. (2014), "Sustainable Building Design," *Journal of Civil Engineering and Management*, Vol. 20, No. 1, pp. 1–10.

Yang, Y.S., Wang, W. and Lin, J.Z. (2017), "Direct–Iterative Hybrid Solution in Nonlinear Dynamic Structural Analysis," *Computer-Aided Civil and Infrastructure Engineering*, Vol. 32, No. 5, pp. 397–411.

Yeganeh-Fallah, A. and Taghikhany, T. (2016), "A Modified Sliding Mode Fault Tolerant Control for Large Scale Civil Infrastructures," *Computer-Aided Civil and Infrastructure Engineering*, Vol. 31, No. 7, pp. 550–561.

Young, K. and Adeli, A. (2014a), "Fundamental Period of Irregular Moment-Resisting Steel Frame Structures," *The Structural Design of Tall and Special Buildings*, Vol. 23, No. 15, pp. 1,141–1,157.

Young, K. and Adeli, A. (2014b), "Fundamental Period of Irregular Concentrically Braced Steel Frame Structures," *The Structural Design of Tall and Special Buildings*, Vol. 23, No. 16, pp. 1,211–1,224.

Young, K. and Adeli, H. (2016), "Fundamental Period of Irregular Eccentrically-Braced Tall Steel Frame Structures," *Journal of Constructional Steel Research*, Vol. 120, pp. 199–205.

Zhang, C., Zhao, F. and Liu, Y. (2010), "Diagrid Tube Structures Composed of Straight Diagonals with Gradually Varying Angles," *The Structural Design of Tall and Special Buildings*, Vol. 21, No. 4, pp. 283–295.